

CrystEngComm

Accepted Manuscript



This is an *Accepted Manuscript*, which has been through the Royal Society of Chemistry peer review process and has been accepted for publication.

Accepted Manuscripts are published online shortly after acceptance, before technical editing, formatting and proof reading. Using this free service, authors can make their results available to the community, in citable form, before we publish the edited article. We will replace this *Accepted Manuscript* with the edited and formatted *Advance Article* as soon as it is available.

You can find more information about *Accepted Manuscripts* in the [Information for Authors](#).

Please note that technical editing may introduce minor changes to the text and/or graphics, which may alter content. The journal's standard [Terms & Conditions](#) and the [Ethical guidelines](#) still apply. In no event shall the Royal Society of Chemistry be held responsible for any errors or omissions in this *Accepted Manuscript* or any consequences arising from the use of any information it contains.

High solubility crystalline hydrates of Na and K Furosemide salts†

U. B. Rao Khandavilli,^a Swarupa Gangavaram,^a N. Rajesh Goud,^b Suryanarayan Cherukuvada,^b S. Raghavender,^a Ashwini Nangia,^{a,b,*} Sulur G. Manjunatha,^c Sudhir Nambiar,^c and Sharmistha Pal,^{c,*}

^a Technology Business Incubator, University of Hyderabad, Prof. C. R. Rao Road, Central University PO, Gachibowli, Hyderabad 500 046, India

^b School of Chemistry, University of Hyderabad, Prof. C. R. Rao Road, Central University PO, Gachibowli, Hyderabad 500 046, India

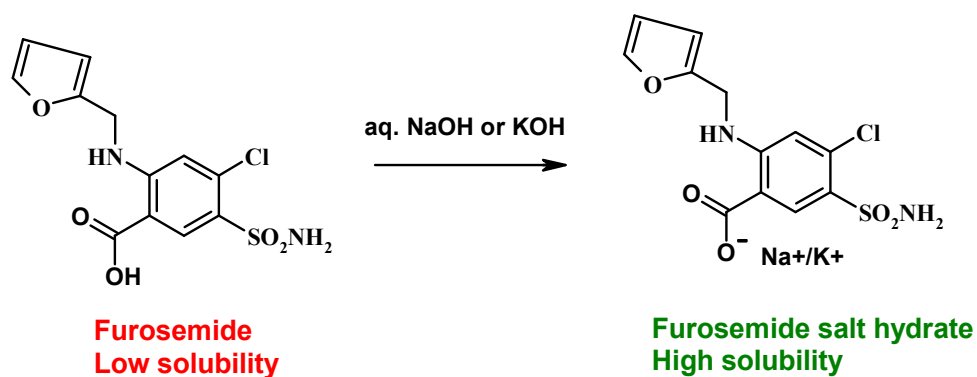
^c Pharmaceutical Development, AstraZeneca India Pvt. Ltd., Bellary Road, Hebbal, Bangalore 560 024, India

E-mail: ashwini.nangia@gmail.com, sharmistha.pal@astrazeneca.com

Abstract

Novel sodium and potassium salts of the poorly soluble loop diuretic drug Furosemide were prepared with the intent of improving drug solubility and bioavailability. Furo-Na salt was obtained as a trihydrate on crystallizing from an aqueous NaOH solution, and Furo-K salt crystallized as a monohydrate from KOH solution. Both the salt hydrates were characterized by X-ray diffraction, DSC, TGA, and IR spectroscopy. An exothermic phase transition at 165 °C in the DSC heating curve of Furo-Na salt indicates the likelihood of polymorphism in its anhydrate phase. Solubility studies on furo-Na-trihydrate and furo-K-monohydrate in pH 7 phosphate buffer medium exhibited significantly higher aqueous solubility of 41 mg/mL and 106 mg/mL compared to the free drug (0.01 mg/mL). The physical stability of these fast dissolving salts under accelerated ICH conditions of 40 °C and 75% RH was modest, with Furo-Na salt being stable for 2 weeks and Furo-K salt surviving for 1 week.

† Electronic Supplementary Information is available with this paper. IR spectra of furo-Na-trihydrate and furo-K-monohydrate (Fig. S1 and S2), Dissolution measurement linear fit plots (Fig. S3), Post solubility/dissolution PXRD patterns (Fig. S4), DVS plots (Fig. S5), and Post DVS PXRD patterns (Fig. S6). Crystallographic .cif files are downloadable from www.ccdc.cam.ac.uk (CCDC Nos. 938492 – 938493).

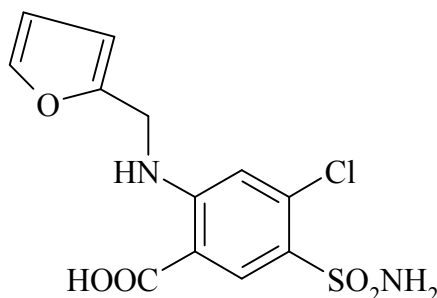


Furosemide is crystallized as Na and K carboxylate hydrate salts and their X-ray crystal structures were determined. Furosemide-Na-trihydrate displayed aqueous solubility of about 4,000 fold higher than that of furosemide and furosemide-K-monohydrate has over 10,000 times improved solubility.

Introduction

The systematic characterization of various solid forms of a drug molecule is crucial for the rational design of dosage forms and selection of optimal conditions for their development and storage¹. Furosemide is a loop diuretic drug approved by the US-FDA in 1982. It is primarily used to treat congestive heart failure and oedema and occasionally for treating hypertension. Furosemide (brand name LASIX) belongs to the Biopharmaceutics Classification System (BCS) class IV of drugs,² i.e. it has low solubility (10 mg/L in water) and low permeability ($\log P_{ow}$ 0.74).³ Low solubility and low permeability are defined for pharmaceuticals as <10 mg/L and $\log P_{ow}$ <1.72, respectively.⁴ The mean bioavailability of Lasix is 60% and the typical daily dose is 20-80 mg while the maximum permissible dose is 600 mg/day. Improving the solubility of furosemide by solid form selection and optimization could result in a high solubility oral formulation of the drug with enhanced bioavailability. Several approaches to modify the physicochemical properties of drugs, e.g. polymorphs, hydrates, amorphous materials, solvates, salts, cocrystals, solid dispersions, encapsulation in cyclodextrins, nanoparticles, etc. are reported in literature.^{5,6,7}

Crystalline forms of furosemide such as polymorphs, solvates⁸⁻¹² as well as salts with amino acids have been reported¹³. Recently, our group studied a few cocrystals and a cytosine salt¹⁴ of furosemide for solubility enhancement, among which furo-cytosine salt and furo-caffeine cocrystal were found to be the most promising candidates, exhibiting 11- and 6-fold higher solubility than the parent drug. However, the limited physical stability of these soluble compounds for no more than 2 days in slurry conditions was a setback towards developing an optimal solid form. The cocrystal forms therefore were not suitable for an improved formulation. Moreover, solubility enhancement through pharmaceutical cocrystals (4–100 fold) is an order of magnitude lower than what is possible for salts (100–1000 fold) relative to the reference drug.¹⁵ Salt formation is the traditional method to enhance the solubility of poorly soluble drug molecules. It is also the preferred modification for drug molecules intended for parenteral administration¹⁶. Therefore, taking advantage of the COOH functional group, we set out to study pharmaceutically acceptable salts of furosemide with inorganic counterions with the intent of improving its solubility with implications of enhanced bioavailability and therapeutic efficacy.^{17,18}



Scheme 1 Chemical structure of furosemide.

Experimental Section

Furosemide (purity >99.8%) was supplied by AstraZeneca India Pvt. Ltd. KOH, NaOH (purity >99.8%) and solvents (purity >99%) were purchased from Hychem Laboratories (Hyderabad). Water filtered through a double deionized purification system (AquaDM, Bhanu, Hyderabad) was used in all experiments.

Preparation of furosemide salt hydrates

Furosemide sodium trihydrate salt 500 mg of furosemide (ca. 1.5 mmol) was dissolved in 5 mL of 5 N NaOH with gentle heating. The resulting solution was left for slow evaporation at ambient conditions. Single crystals of furosemide sodium trihydrate salt suitable for X-ray diffraction were obtained after 7 days. The resulting material was filtered and left to dryness. Several experiments following the same procedure were repeated to produce the crystalline salt hydrate in bulk amount for further characterization and measurements.

Furosemide potassium monohydrate salt 500 mg of furosemide (ca. 1.5 mmol) was dissolved in 5 mL of 5 N KOH with gentle heating. The resulting solution was left for slow evaporation at ambient conditions. Single crystals of furosemide potassium monohydrate salt suitable for X-ray diffraction were obtained after 7 days. The resulting material was filtered and left to dryness. Several experiments following the same procedure were repeated to produce the crystalline salt hydrate in bulk amount for further characterization.

Powder X-ray diffraction

Powder X-ray diffraction of all samples were recorded at 298 K on a D8 Focus diffractometer (Bruker-AXS, Karlsruhe, Germany) using Cu-K α X-radiation ($\lambda = 1.5406 \text{ \AA}$) at 40 kV and 30 mA power. X-ray diffraction patterns were collected over the 2θ range $5\text{-}50^\circ$ at a scan rate of $1^\circ/\text{min}$.

Single crystal X-ray diffraction

X-ray reflections were collected on an Xcalibur Gemini EOS CCD diffractometer (Oxford Diffraction, Yarnton, UK) using Mo-K α , radiation at 298 K. Data reduction was performed using CrysAlisPro (version 1.171.33.55). OLEX2-1.0,¹⁹ and SHELX-TL 97²⁰ were used to solve and refine the reflections data. Non hydrogen atoms were refined anisotropically. Hydrogen atoms on N and O were located from difference electron density maps and C-H hydrogens were fixed using the HFIX command in SHELX-TL.²⁰

Thermal analysis

Differential scanning calorimetry was performed on DSC 822e module, and TGA was performed on TGA/SDTA 851e module (Mettler-Toledo, Columbus, USA). Samples were placed in open alumina pans for TG experiments and in crimped but vented aluminum pans for DSC experiments. A typical sample size was 3-5 mg for DSC and 8-12 mg for TGA. The temperature range for the measurement was 30-350 °C and the sample was heated at a rate of 5°C/ min. Samples were purged in a stream of dry nitrogen flow at 80 mL/ min for DSC and 50 mL/ min for TGA.

IR spectroscopy

FT-IR 6700 spectrometer (Thermo-Nicolet, Waltham, USA) was used to record IR spectra with the samples dispersed in KBr pellets. Data were analyzed using the Omnic software (Thermo Scientific, Waltham, USA).

Physical stability of solid forms

About 200 mg of each solid compound was placed in an open petri dish and stored in a T-90S stability chamber (Thermolab Scientific, Mumbai, India) pre-maintained at 40 °C and 75% RH (accelerated

conditions as per WHO/ICH guidelines)²¹ for 3 weeks. The physical stability of the solid forms and integrity of the samples was assessed periodically by PXRD.

Dissolution and solubility

The solubility curves of Furosemide salts were measured using the Higuchi and Connor method²² in phosphate buffer of pH 7 ($\text{Na}_2\text{HPO}_4 + \text{KH}_2\text{PO}_4$) at 30 °C. First, the absorbance of a known concentration of the salt was measured at the given λ_{max} (230 nm) on Evolution 300 UV-vis spectrometer (Thermo Scientific, Waltham, USA). These absorbance values were plotted against several known concentrations to prepare the concentration vs. intensity calibration curve. From the slope of the calibration curves, molar extinction coefficients of furosemide salts were calculated. In order to determine the equilibrium solubility, an excess amount of salt hydrate was added to 6 mL of phosphate buffer. The supersaturated solution was stirred at 50 rpm using a magnetic stirrer at 30°C. After 24 h, the suspension was filtered through Whatman's 0.45 micron syringe filter. The filtered aliquots were diluted, and the absorbance was measured at the given λ_{max} . IDR (Intrinsic Dissolution Rate) experiments were carried out on USP-certified TDT-08L dissolution tester type II apparatus (paddle) (Electrolab, Mumbai, India). Dissolution experiments were performed in 10% ethanol–water (for furosemide) and phosphate buffer (for salt hydrates) at 30 °C for 24 min. For IDR measurements, 500 mg of the compound was taken in the intrinsic attachment and compressed to 0.5-cm² disk using a hydraulic press at 4.0 ton/in² pressure for 5 min. The intrinsic attachment was placed in a jar of 900 mL medium preheated to 30°C and rotated at 50 rpm. 5 mL of the aliquot was collected at specific time intervals, and the concentration of the aliquots was determined with appropriate dilutions from the predetermined standard curves of the respective compounds. The IDR of the compound was calculated in the linear region of the dissolution curve (which is the slope of the curve or the amount of drug dissolved/surface area of the disk) per unit time. Any possible phase transformations during the dissolution experiments and/or disk compression were monitored by PXRD of the residue.

Dynamic vapor sorption (DVS) study

DVS measurements were performed on Q5000SA vapor sorption Analyzer (TA Instruments, Delaware, USA) at 40 °C. About 5 mg of the sample was placed in a metallic-quartz sample pan and subjected to relative humidity flux from 10 to 90% and back to 10% RH with a step size of 10% change in humidity. A dwell time of 60 min was set for weight change of >0.1% in the adsorption/desorption phase at a particular RH (5 min dwell time for weight change of <0.1%). Thus, if the weight loss/gain is >0.1% at a particular RH, the instrument maintains the same RH for 60 min and then automatically sets at the next higher/lower value. If the weight gain/loss is < 0.1 %, DVS cycle (10-90-10%) will complete within 2 hours, otherwise it will take longer duration.

Results and Discussion

Salt formation is the classic method for improving the solubility and filterability of acidic and basic drugs. The Orange book database lists various drug products approved by the US-FDA,²³ and the frequency of counterions used for salt formation over different decades. Sodium is the most preferred cation for salt formation (75.3%) followed by calcium (6.9%) and potassium (6.3%). Among anions, chloride has a high percentage of usage (54.3%) followed by sulfate (7.2%). These statistics not only support the widespread use of Na^+ and Cl^- counterions in pharmaceutical salts but also hint at the solubility advantage conferred by them.^{24,25} Our experiments to obtain Furosemide salts with these counterions resulted in sodium and

potassium salts as crystalline furo-Na-trihydrate and furo-K-monohydrate (see X-ray crystal data in Table 1 and hydrogen bonds metrics in Table 2).

Table 1 Crystal structure parameters of Furo-Na-trihydrate and Furo-K-monohydrate.

	Furo-Na-trihydrate	Furo-K-monohydrate
Empirical formula	C ₁₂ H ₁₆ Cl N ₂ O ₈ S Na	C ₁₂ H ₁₂ Cl N ₂ O ₆ S K
Chemical formula	(C ₁₂ H ₁₀ Cl N ₂ O ₅ S Na). 3(H ₂ O)	(C ₁₂ H ₁₀ Cl N ₂ O ₅ S K). (H ₂ O)
Formula weight	406.77	386.85
Crystal system	monoclinic	monoclinic
Space group	<i>P2₁/c</i>	<i>P2₁/c</i>
T (K)	298(2)	298(2)
a (Å)	20.9184(10)	18.8967(10)
b (Å)	10.4771(6)	11.1734(6)
c (Å)	7.8468(4)	7.3056(4)
α (°)	90	90
β (°)	95.790(4)	91.346(5)
γ (°)	90	90
Z	4	4
Volume (Å ³)	1710.96(15)	1542.08(15)
R ₁	0.0476	0.0752
wR ₂	0.0901	0.2326
GOF	0.920	1.183

Table 2 Hydrogen bond distances and angles in Furosemide salt hydrates (N–H 1.009 Å, O–H 0.983 Å, and C–H 1.083 Å distances were neutron-normalized).

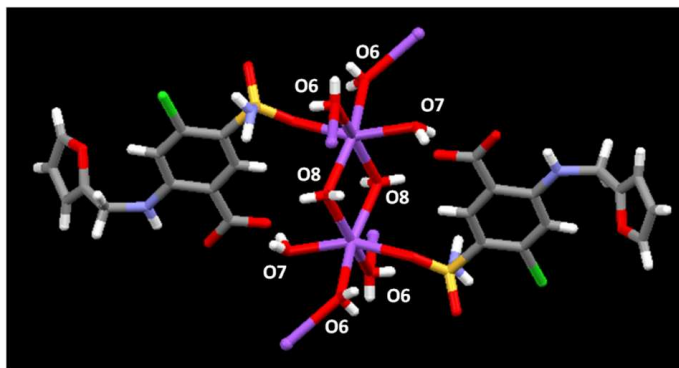
D–H⋯A	D⋯A (Å)	H⋯A (Å)	D–H⋯A (°)	symmetry code
Furo-Na-trihydrate				
N1–H1A⋯O2	2.910(4)	2.21	126	x, –1/2–y, 1/2+z
N1–H1B⋯O4	2.798(4)	1.84	158	x, 1/2–y, 1/2+z
N2–H2⋯O4	2.660(4)	1.86	134	--- ^a
O6–H6A⋯O4	2.933(4)	2.06	146	x, –1+y, z

O7–H7A···O3	2.760(4)	1.78	171	1-x, -y, 1-z
O7–H7B···O3	2.784(4)	1.83	163	1-x, -1/2+y, 1/2-z
O8–H8A···O7	2.802(4)	1.82	173	1-x, 1/2+y, 1/2-z
O8–H8B···O3	2.917(4)	1.96	162	1-x, -1/2+y, 1/2-z
Furo-K-monohydrate				
N1–H1A···O4	2.846(9)	1.85	168	x, 1/2-y, -1/2+z
N1–H1B···O2	2.923(10)	2.13	134	x, 3/2-y, -1/2+z
N2–H2···O4	2.643(7)	1.84	134	--- ^a
O6–H6A···O3	2.791(8)	1.81	176	1-x, -y, -z
O6–H6B···O3	2.835(8)	1.86	173	1-x, -1/2+y, 1/2-z

^a Intramolecular hydrogen bond

Characterization of furosemide-sodium trihydrate

Single crystal X-ray diffraction of furo-Na-trihydrate salt confirmed the constituents of the unit cell as one furosemide-CO₂⁻, one Na⁺, and three water molecules. The Na⁺ ion exhibits an octahedral environment through coordinate covalent bonds with O1 of SO₂NH₂ (2.03 Å) and three water molecules (O6, O7, O8) as shown in Fig. 1. The cation is not coordinated to the carboxylate group, perhaps due to the steric hindrance arising as a result of stronger coordination to the SO₂NH₂ and 5 water molecules around each Na⁺. O7 water molecule acts as a non-bridging molecule to Na⁺ ion, and O6, O8 water molecules form a (6,3)-net as bridging molecules. The carboxylate O3 and O4 atoms form trifurcated interactions with different hydrogen bond donors. While O3 forms hydrogen bonds with O7 (O7–H7A···O3, 1.78 Å, 171° and O7–H7B···O3, 1.83 Å, 163°) and O8 (O8–H8B···O3, 1.96 Å, 162°) water molecules, O4 participates in an intramolecular hydrogen bond with the amine N-H (N2–H2···O4, 1.86 Å, 134°), and an interaction with sulfonamide N-H (N1–H1B···O4, 1.84 Å, 158°) and O6 water (O6–H6A···O4, 2.06 Å, 146°). This one-point hydrogen bonding interaction between O6 and O4 extend the coordination polymer like octahedral moieties unidimensionally along *b*-axis (Fig. 2). The sulfonamide NH₂ is bonded in a catemer chain with S=O acceptor (N1–H1A···O2, 2.21 Å, 126°).



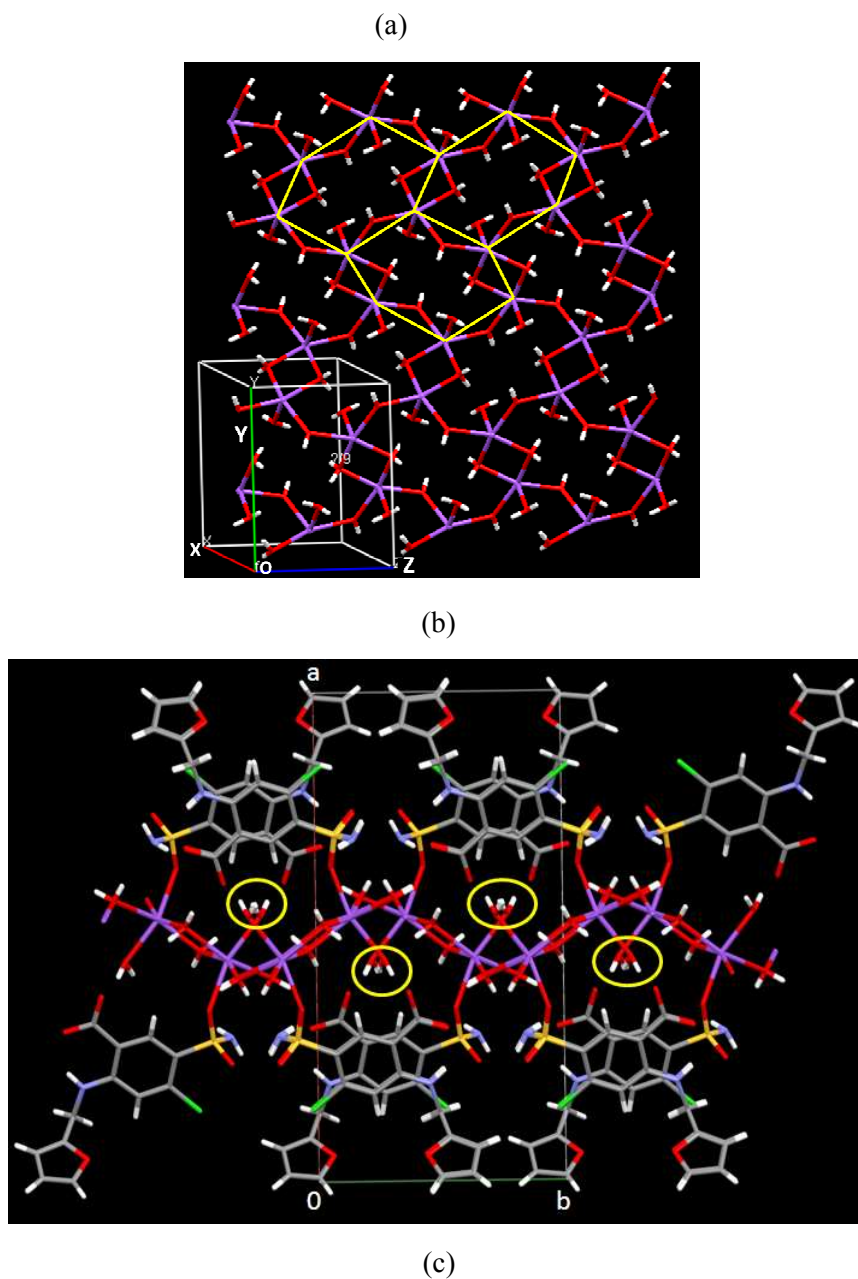


Fig. 1 Crystal structure of furosemide-Na-trihydrate. (a) A sodium ion is coordinated to five water molecules and one oxygen atom of the sulfonamide group of furosemide in an octahedral environment. (b) The arrangement of water molecules with the sodium ion at the octahedral center. Two water molecules (O6 and O8) form a (6,3)-net (shown in yellow line) and act as bridging molecules. The third water (O7) is a non-bridging molecule. (c) Detailed view of the third water molecule (O7) attached to the network above and below by sitting crisscross in the channel (yellow circle) of the crystalline hydrate.

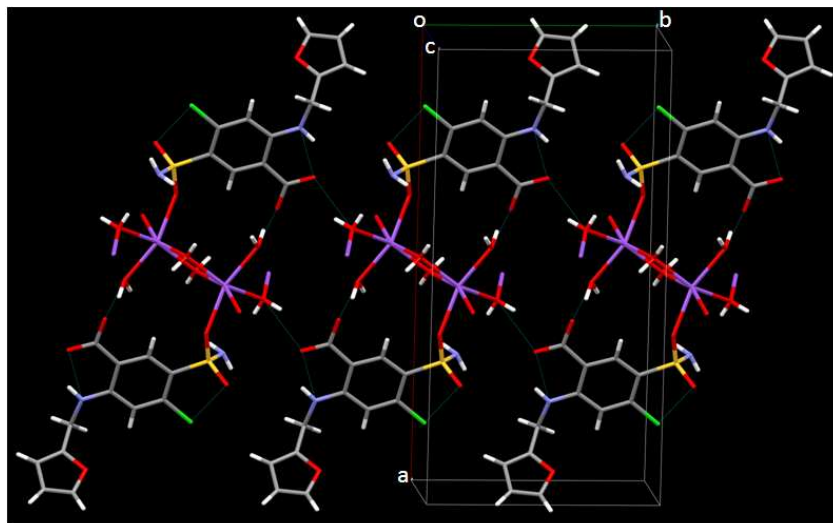


Fig. 2 Hydrogen bonding of water donors and sulfonamide NH to the carboxylate COO^- acceptors O3 and O4 in furo-Na-trihydrate.

The furosemide Na salt trihydrate bulk material was characterized by PXRD (Fig. 3). The experimental PXRD pattern of the salt hydrate showed a good match with its calculated diffraction line pattern. The water stoichiometry of the salt hydrate was also confirmed by DSC and TGA experiments (Fig. 4). DSC showed three endotherms at 69 °C, 88 °C and 127 °C and correspondingly three weight loss steps were observed in TGA with total weight loss matching the trihydrate stoichiometry (obsd. 12.92%, trihydrate calc. 13.24%). The DSC heating curve showed an additional minor exotherm (4.9 kJ/mol) at 165 °C (before the major decomposition exotherm at 265 °C) corresponding to a likely polymorphic phase transition of the furosemide sodium salt anhydrate (dehydration of the hydrate in the DSC pan after water loss). This was confirmed by the difference in the PXRD patterns of the sodium salt anhydrate obtained upon controlled heating of trihydrate material before (at 150 °C) and after (at 190 °C) the exotherm (Fig. 4). However the transformation appears to be incomplete as analyzed by PXRD (Fig. 5). Heat-cool-heat DSC experiment on the trihydrate sample showed that the exotherm is not reversible during the cooling cycle and on reheating it showed a single melting endotherm followed by decomposition peak characteristic of furosemide (Fig. 6). Further experiments are ongoing to isolate and characterize these anhydrous salt polymorphs and study their thermal stability relationship. The IR spectrum of furo-Na-trihydrate is shown in Fig. S1 (ESI†).

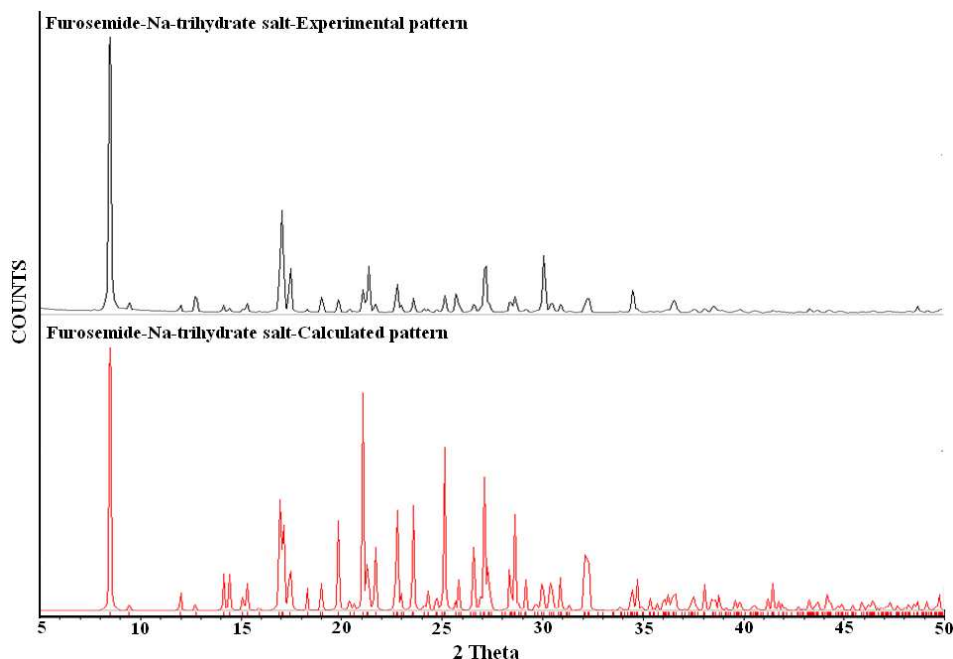


Fig. 3 Stacked PXRD of furo-Na-trihydrate. The experimental line pattern (black) showed good match with the calculated lines from the X-ray crystal structure of the trihydrate (red), indicating bulk purity.

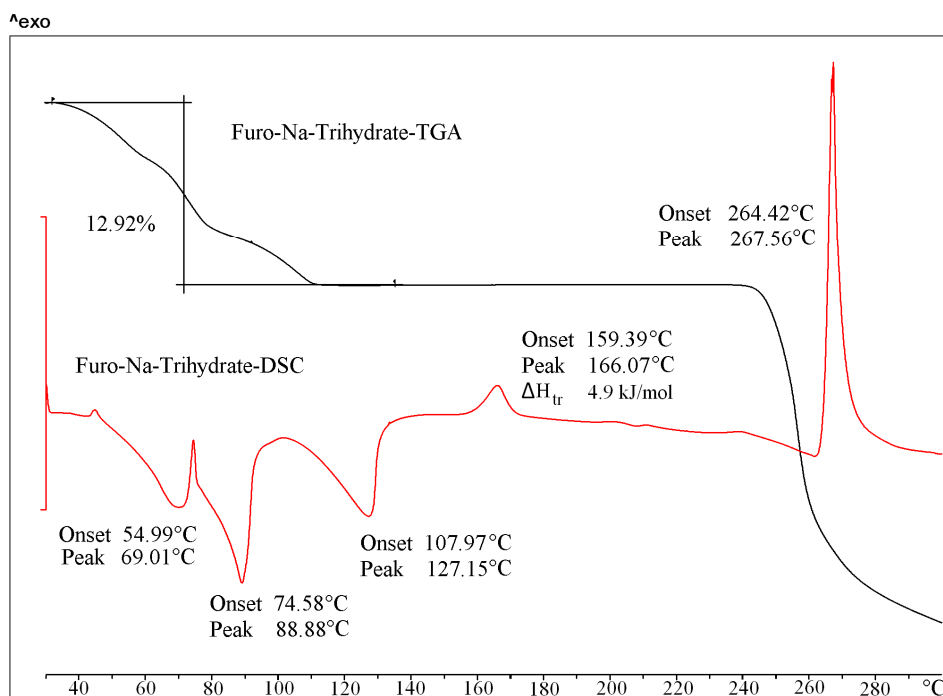


Fig. 4 Overlay of DSC and TGA heating curves of Furo-Na-trihydrate matched well with the water stoichiometry observed in the crystal structure.

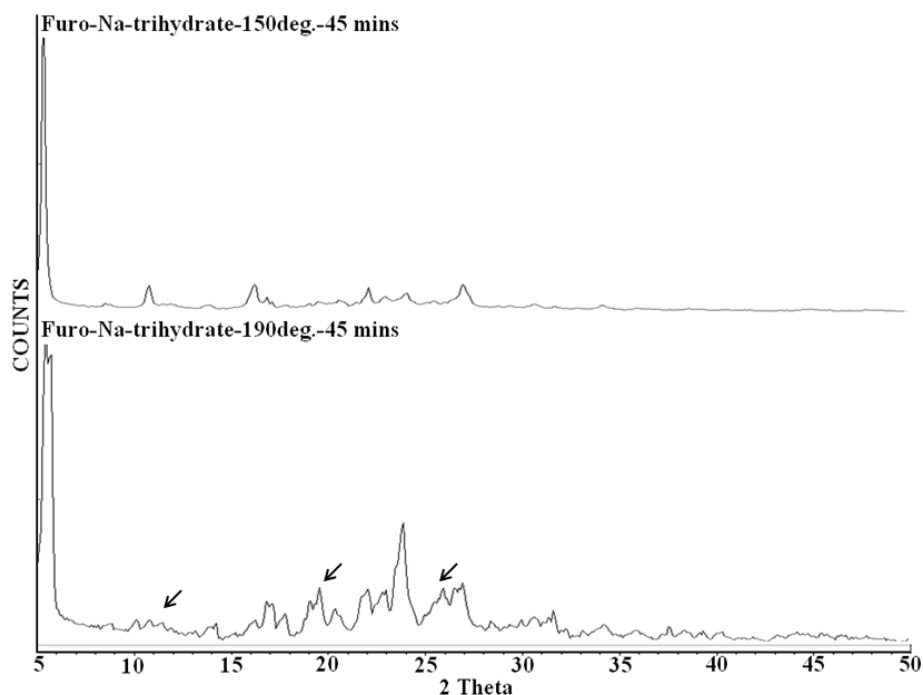


Fig. 5 Stacked PXRD patterns of furosemide-Na-trihydrate at 150°C and 190°C (below and above the exotherm T at ~165 °C) indicate polymorphism of the anhydrate. The new peaks are marked with an arrow to show the phase change.

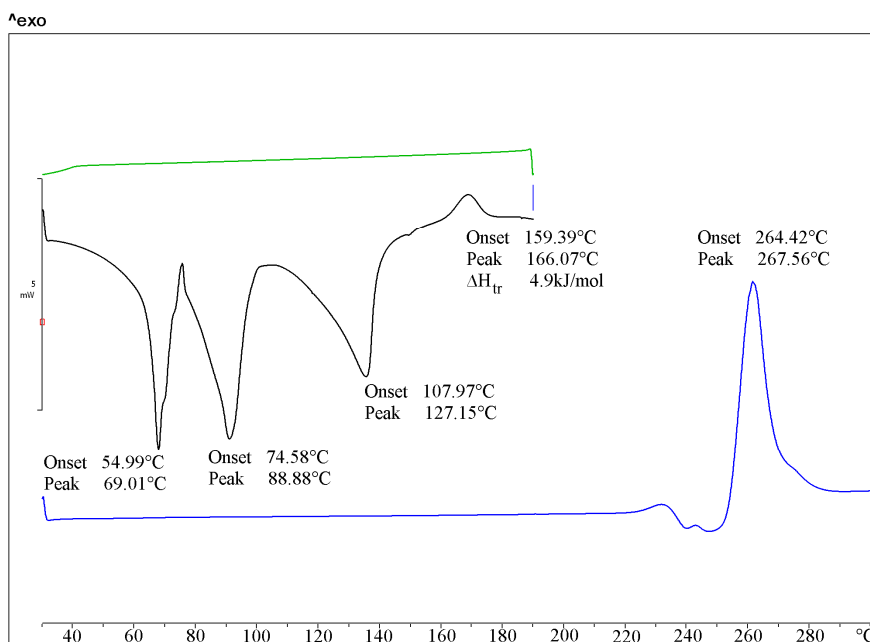


Fig. 6 Heat-cool-reheat DSC on furosemide showed that the exotherm at 165 °C is not reversible during the cooling cycle and the reheating run showed a single melting followed by the decomposition peak characteristic of furosemide.

Characterization of Furosemide-potassium monohydrate

The asymmetric unit of this crystal structure contains one furosemide-CO₂⁻, one K⁺, and one water molecule. Here the K atom is eight-coordinated, being bonded to O3, O4 (carboxylate chelate), O1, O2 (sulfonamide, 2 moieties), and O6 (2 water molecules). The water donors are bonded to carboxylate O3 acceptors in this monohydrate structure (O6-H6A...O3, 1.81 Å, 176°, O6-H6B...O3, 1.86 Å, 173°) (Fig. 7). The PXRD of the bulk material showed a diffraction pattern that matched well with the furo-K-monohydrate calculated diffraction line pattern up to 2θ = 30° (Fig. 8). The endotherm for water loss in DSC and the percentage weight loss in TGA are consistent with a single water molecule in the crystal structure (obsd. 4.03%; calc, 4.66%) as shown in Fig. 9. The IR spectrum of furo-K-monohydrate is shown in Fig. S2, ESI†.

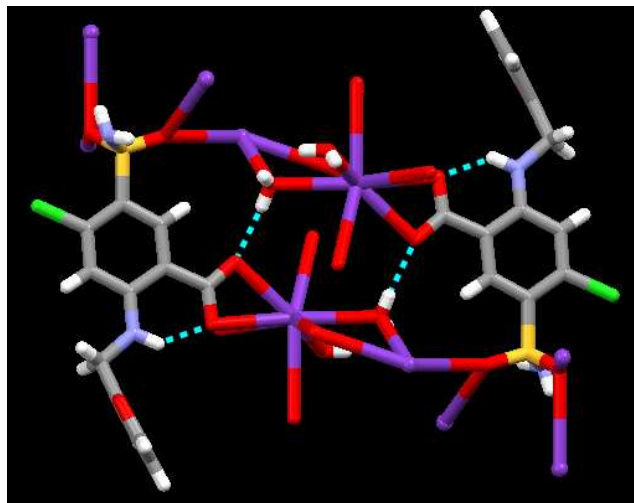


Fig. 7 Crystal structure of furo-K-monohydrate shows a 1:1:1 K : furosemide : H₂O stoichiometry in the salt hydrate.

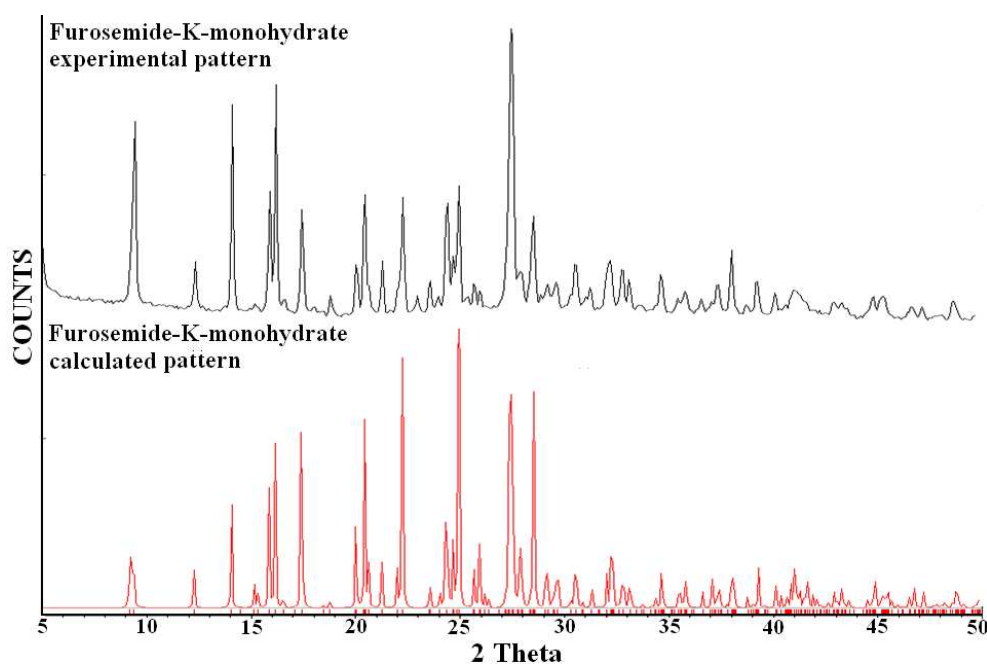


Fig. 8 Overlay of the best experimental PXRD of furo-K-monohydrate (black) with calculated lines from the X-ray crystal structure of furo-K-monohydrate (red).

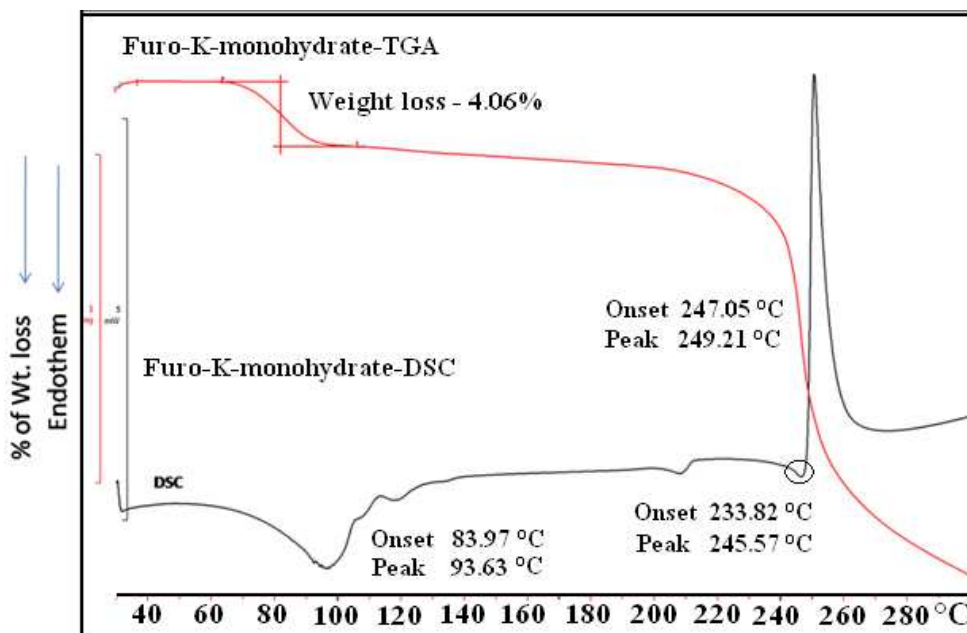


Fig. 9 DSC and TGA of furo-K-monohydrate show a single endotherm for water loss (one molecule) at 90-100 °C. The compound shows a minor melting peak (indicated by a circle) at 245 °C followed by the major decomposition peak at 255 °C.

Solubility and Dissolution

The optimization of physicochemical parameters of a drug molecule is essential for better therapeutic efficacy and drug-patient compatibility. Poor solubility remains a major concern for BCS class II and class IV drug molecules since it largely limits their bioavailability. Hence physical or chemical modifications are essential for such drugs to improve their solubility and efficacy. Solubility and dissolution studies were carried out on Furosemide (a BCS class IV drug) salt hydrates in order to evaluate their solubility advantage. Solubility is a thermodynamic parameter of “how much” of the solute dissolves in a given solvent at equilibrium conditions (usually 24–48 h). Equilibrium solubility experiments on furosemide salt hydrates were performed in pH 7 phosphate buffer for 24 h. During the course of equilibrium solubility experiments, furosemide and its salt hydrates were found to be stable as confirmed by PXRD of the solid residue remaining at the end of the experiment. Since there was no evidence of solid form conversion for extended periods of time, the solubility numbers may be used as a reliable guide to estimate the higher solubility of salt hydrates compared to the pure drug. The solubility of these salt hydrates is superior to that of the pure drug. The solubility of furo-Na-dihydrate is about 4,000 times greater than that of pure furosemide. The solubility of furo-K-monohydrate is 2.6 times greater than furo-Na-dihydrate, or 10,600 fold higher than that of free furosemide (Table 3).

Dissolution is a particularly useful measure for solid APIs undergoing phase transformation during solubilization (e.g. polymorphic transformation, hydrate formation, etc.).^{6b} For such APIs, the IDR during early time periods (15 min to a few hours) is a more helpful parameter than equilibrium solubility because phase changes may have occurred (e.g. to hydrate form) before the equilibrium value is reached. Thus, dissolution studies are more informative for metastable drug forms.²⁶ Given the very high solubility of the salts, dissolution experiments were performed for 30 min only. The equilibrium solubility at 24 h and the dissolution rate from the linear region of the IDR curves (Fig. 10) are listed in Table 3. Linear fit dissolution data points used to calculate IDR of the respective compounds are shown in Figure S3. Because the solubility of furosemide is very low in water (10 mg/L), obtaining a UV-Vis standard curve was not possible in aqueous buffer medium. Hence, the extinction coefficient of furosemide was determined in 10% EtOH–water solution and that of salts in pH 7 phosphate buffer. PXRD patterns of furosemide and its salt hydrates at the end of solubility/dissolution experiments resemble the starting materials indicating physical form stability (Fig. S4).

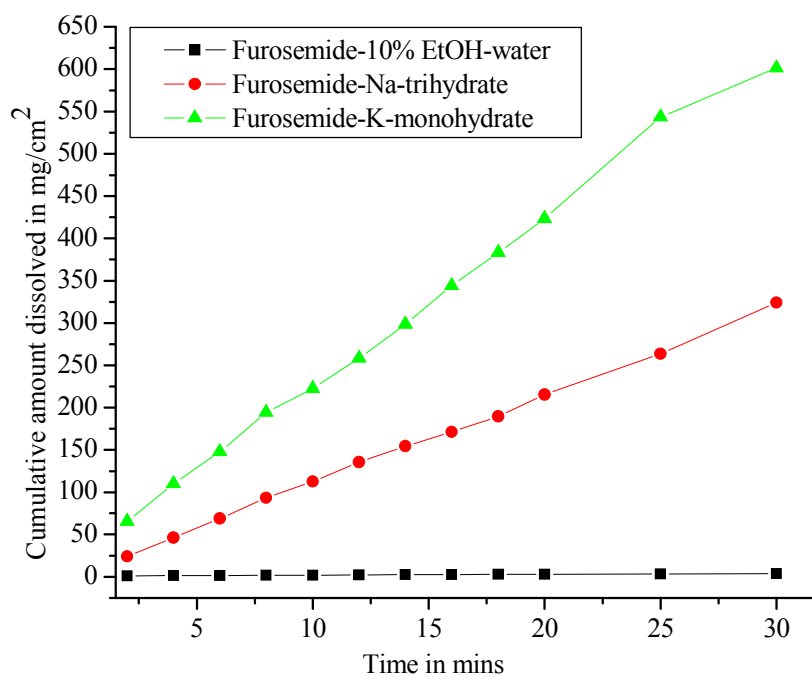


Fig. 10 Dissolution of furo-Na-trihydrate and furo-K-monohydrate salts in phosphate buffer pH 7 and that of furosemide in 10% EtOH–water (solubility 3 mg/mL).

Table 3 Solubility and dissolution rates of furosemide salt hydrate.

Compound	Solubility in pH 7 phosphate buffer (at 24 h) (mg/mL) (X no of times)	IDR in pH 7 phosphate buffer (mg/cm ²)/ min)	Physical Stability in medium

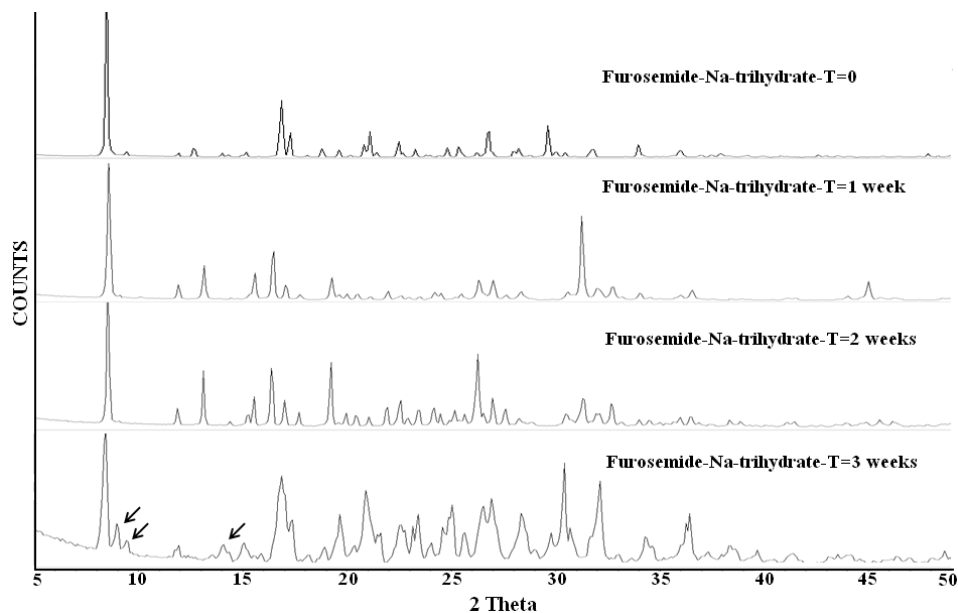
	increment)		
Furosemide	0.01 ^a	0.28 in 10% EtOH–Water) (0.2)	Stable (also in 10% EtOH–water medium for dissolution)
Furosemide-Na- trihydrate	40.5 (±3.9) (x 4050)	11.9 (±3.6)	Stable
Furosemide-K- monohydrate	106.4 (±5.3) (x 10640)	26.3 (±5.3)	Stable

^a <http://166.78.14.201/tsrlinc.com/services/bcs/results.cfm>

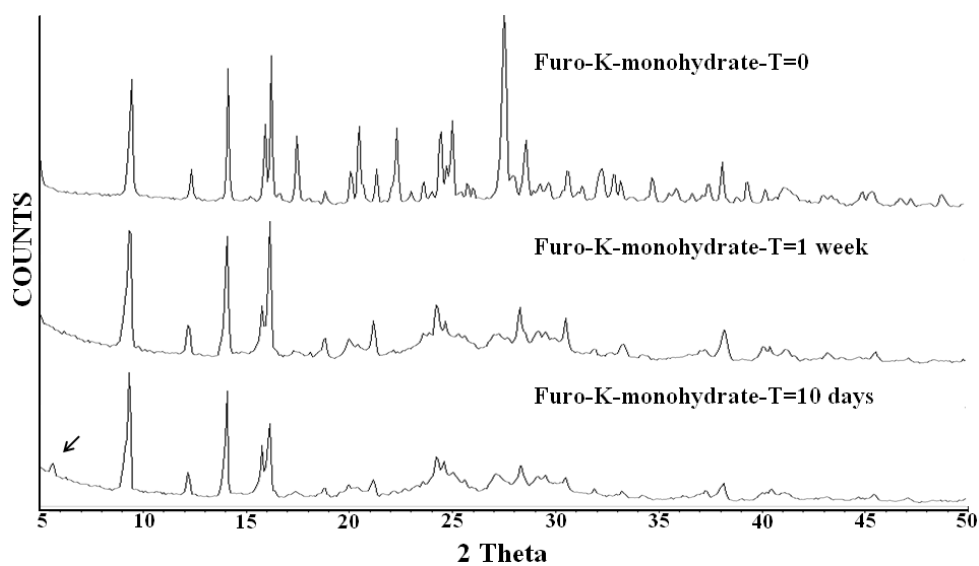
Is the solubility and dissolution rate enhancement an artifact of pH speciation behavior due to furosemide salt added? It is well known that aqueous phosphate ($\text{Na}_2\text{HPO}_4 + \text{KH}_2\text{PO}_4$) in the buffer medium will set up local equilibrium of ion pairs, H_3PO_4 , H_2PO_4^- , HPO_4^{2-} , PO_4^{3-} , at $\text{pK}_a \approx 2, 7, 13$ (half neutralization point). Hence the carboxylate Na salt of furosemide ($\text{pK}_a 3.5\text{--}4.0$) will not significantly alter the pH of the buffer medium since the region in which the acid is in equilibrium with its conjugate base is $\text{pH} \approx \text{pK}_a \pm 2$. In the idealized situation of constant ionic strength, the three buffering zones for phosphate buffer are pH 0–4, 5–9, 10–14. The pH of the medium during the entire solubility experiment was constant at about $\text{pH} \approx 7$ (no change).

Physical stability of furosemide salt hydrates

Furosemide salt hydrates were kept at accelerated ICH conditions of 40 °C and 75% RH and PXRDs were recorded periodically over 1 month. While furo-Na-trihydrate was stable for 2 weeks after which it started converting to a new solid modification which could possibly due to its conversion to monohydrate or dihydrate phases as confirmed by the peaks in the PXRD pattern at 2θ of 7, 9 and 15°, Furo-K-monohydrate was stable for 1 week after which it showed conversion to furosemide as evidenced by the characteristic 2θ peak at 6° (Fig. 11).



(a)



(b)

Fig. 11 (a) Furo-Na-dihydrate kept at accelerated ICH conditions of 40 °C and 75% RH was stable for 2 weeks, but new peaks appeared at 3 weeks. (b) Furo-K-monohydrate under the same conditions was stable for 1 week and then started converting to furosemide. The small peak at about 6° 2θ for furosemide starts to appear in the 10 d plot.

Dynamic Vapor sorption

Dynamic vapor sorption (DVS) was used to obtain sorption–desorption kinetics of furosemide salt hydrates. The adsorption–desorption isotherm of Furo-Na-trihydrate is a case of simple moisture

adsorption²⁷ rather than molecular bound water since the adsorption–desorption cycles were reversible without any hysteresis. Between 10-70 % RH the trihydrate salt was stable and did not uptake any significant water in this range. Above 70% RH the salt adsorbed up to 48.7% water (see Fig. S5a) up to 90% RH. During desorption cycle, the material lost 48.7% of water which means that it converted back to the trihydrate at 10% RH.

Vapor sorption studies on Furo-K- monohydrate were similar to the adsorption-desorption cycle of furo-Na-trihydrate since it showed steep water adsorption above 70% RH and exhibited gain of 4.8% water content at 90% and upon desorption did not retain any water in the crystal lattice (Fig. S5b). This appears to be a case of simple surface adsorption. Samples at the end of the DVS experiment did not show phase conversion as observed by PXRD analysis (Fig. S6).

Conclusions

Furosemide is a classic diuretic drug for the treatment of hypertension and oedema. However, its low solubility (0.01 mg/mL) is a limiting factor for good bioavailability of the oral dose. Driven with an aim to enhance solubility, we prepared Na and K salt hydrates of furosemide. Both these novel hydrates were characterized by thermal, spectroscopic and diffraction techniques. In addition, the physical stability and hydration behavior of these salt forms was analyzed using DVS. The significantly enhanced solubility of 40 mg/mL and 106 mg/mL for furo-Na-trihydrate and furo-K-monohydrate, respectively, compared to the free drug (0.01 mg/mL) establishes the high solubility of these salt hydrates. Sodium salts have been used as excipients with furosemide.²⁸ In-house studies at accelerated ICH conditions of 40 °C and 75% RH of the Na and K salts hydrates showed good physical stability for 2 weeks and 1 week, respectively. Thus relatively simple and inexpensive Na and K salt hydrates of furosemide described in this study provide leads to develop improved furosemide formulation.

Acknowledgements

AN thanks the DST (JC Bose Fellowship SR/S2/JCB-06/2009), CSIR (Pharmaceutical Cocrystals Project 01/2410/10/EMR-II), and DST-SERB (Novel Solid-state Forms of APIs, SR/S1/OC-37/2011) for research funding. DST (IRPHA) and UGC (PURSE grant) are thanked for providing instrumentation and infrastructure facilities at UoH. N.R.G. and S.C. thank the CSIR and ICMR for fellowship. Crystallin Research thanks AstraZeneca (India) for sponsoring a research project at TBI-UoH.

References

1. S. R. Byrn, In *Solid-State Chemistry of Drugs*, Academic Press, New York, 1982.
2. (a) P. A. Friedman and W. O. Berndt, In *Modern Pharmacology With Clinical Applications*, Ed. C. R. Craig and R. E. Stitzel, Little Brown and Company, Boston, MA, 5th Edn., 1997, pp. 239-255; (b) M. G. Khan, In *Encyclopedia of Heart Diseases*, Elsevier, New York, 15th Edn., 2006, p. 486.
3. <http://166.78.14.201/tsrlinc.com/services/bcs/results.cfm> (accessed on 27 December 2013).
4. <http://www.fda.gov/AboutFDA/CentersOffices/OfficeofMedicalProductsandTobacco/CDER/uem128219.htm> (accessed on 27 December 2013)
5. (a) S. Datta and D. J. W. Grant, *Nat. Rev.*, 2004, **3**, 42; (b) S. L. Morissette, S. Souasene, D. Levinson, M. J. Cima and O. Almarsson, *Proc. Natl. Acad. Sci. U.S.A.*, 2003, **100**, 2180; (c) O. Almarsson, M. B. Hickey, L. Peterson, S. L. Morissette, S. Soukasene, C. McNulty, M. Tawa, J. L. MacPhee and J. F. Remenar, *Cryst. Growth Des.*, 2003, **3**, 927; (d) S. R. Byrn, R. R. Pfeiffer and J. G. Stowell in *Solid-State Chemistry of Drugs*, SSCI, West Lafayette, IN, 1999.
6. (a) J. Bernstein, In *Polymorphism in Molecular Crystals*, Clarendon, Oxford, U. K., 2002; (b) R. Hilfiker, In *Polymorphism in the Pharmaceutical Industry*, Wiley-VCH, Weinheim, Germany, 2006; (c) A. J. Matzger, Ed. Special Issue on Facets of Polymorphism in Crystals, *Cryst. Growth Des.* 2008, **8**, 2-161.
7. (a) S. L. Childs and M. J. Zaworotko, *Cryst. Growth Des.*, 2009, **9**, 4208; (b) N. Shan and M. J. Zaworotko, *Drug Disc. Today*, 2008, **13**, 440; (c) O. Almarsson and M. J. Zaworotko, *Chem. Commun.*, 2004, 1889; (d) S. L. Morissette, O. Almarsson, M. L. Peterson, J. F. Remenar, M. J. Read, A. V. Lemmo, S. Ellis, M. J. Cima and C. R. Gardner, *Adv. Drug Delivery Rev.*, 2004, **56**, 275; (e) T. Vasconcelos, B. Sarmiento and P. Costa, *Drug Disc. Today*, 2007, **12**, 1068; (f) T. Loftsson and M. E. Brewster, *J. Pharm & Pharmacol.*, 2010, **62**, 1607; (g) A. Fahr and X. Liu, *Expert Opin. Drug Deliv.*, 2007, **4**, 403.
8. C. Doherty and P. York, *Int. J. Pharm.*, 1988, **47**, 141.
9. Y. Matsuda and E. Tatsumi, *Int. J. Pharm.*, 1990, **60**, 11.
10. M. Ge, G. Liu, S. Ma and W. Wang, *Bull Korean Chem. Soc.*, 2009, **30**, 2265.
11. S. Karami, Y. Li, D.S. Hughes, M.B. Hursthouse, A.E. Russell, T.L. Threlfall, M. Claybourn and R. Roberts, *Acta Crystallogr., Sect. B*, 2006, **62**, 689.
12. N. J. Babu, S. Cherukuvada, R. Thakuria and A. Nangia. *Cryst Growth Des.*, 2010, **10**, 1979.
13. R. L. Pellegata, US Patent 5182300, 1990.
14. N. R. Goud, S. Gangavaram, K. Suresh, S. Pal, S. G. Manjunatha, S. Nambiar and A. Nangia, *J. Pharm. Sci.*, 2012, **101**, 664.
15. N. Schultheiss and A. Newman, *Cryst. Growth Des.*, 2009, **9**, 2950.
16. (a) S. M. Berge, L. D. Bighley and D. C. Monkhouse, *J. Pharm. Sci.*, 1977, **66**, 1; (b) S. Sweetana and J. M. Akers, *J. Pharm. Sci. Tech.*, 1996, **50**, 330.

17. J. F. Remenar, M. D. Tawa, M. L. Peterson, O. Almarsson, M. B. Hickey and B. M. Foxman, *CrystEngComm*, 2011, **13**, 1081.
18. W. Ong, E. Y. Cheung, K. A. Schultz, C. Smith, J. Bourassa and M. B. Hickey, *CrystEngComm*, 2012, **14**, 2428.
19. O. V. Dolomanov, L. J. Bourhis, R. J. Gildea, J. A. K. Howard and H. Puschmann, *J. Appl. Crystallogr.*, 2009, **42**, 339.
20. G. M. Sheldrick, SHELX-97, *Program for the Solution and Refinement of Crystal Structures*, University of Göttingen: Göttingen, Germany, 1997.
21. http://www.ich.org/fileadmin/Public_Web_Site/ICH_Products/Guidelines/Quality/Q1F/Stability_Guideline_WHO.pdf (accessed on 18 December 2013)
22. T. Higuchi and K. A. Connors, *Adv. Anal. Chem. Instrum.*, 1965, **4**, 117-212.
23. G. S. Paulekuhn, J. B. Dressman and C. Saal, *J. Med. Chem.*, 2007, **50**, 6665.
24. L. R. Chen, V. G. Young, Jr, D. Lechuga-Ballesteros and D. J. Grant, *J. Pharm. Sci.*, 1999, **88**, 1191.
25. R. Khankari, L. Chen and D. J. Grant, *J. Pharm. Sci.*, 1998, **87**, 1052.
26. J. B. Dressman, G. L. Amidon, C. Reppas and V. P. Shah, *Pharm. Res.* 1998, **15**, 11.
27. M. Aucamp, N. Stieger, N. Barnard, W. Liebenberg, *Int. J. Pharm.*, 2013, **449**, 18.
28. G. E. Granero, M. R. Longhi, M. J. Mora, H. E. Gunginger, K. K. Midha, V. P. Shah, S. Stavchansky, J. B. Dressman and D. M. Barends, *J. Pharm. Sci.*, 2010, **99**, 2544.